

Next Generation Memristor Reservoir Computing

Original

Next Generation Memristor Reservoir Computing / Nikiruy, K.; Ivanov, T.; Ziegler, M.; Rossetti, D.; Corinto, F.; Ascoli, A.; Tetzlaff, R.; Demirkol, A. S.; Schmitt, N.. - (2024), pp. 912-917. (Intervento presentato al convegno 2024 IEEE International Conference on Metrology for eXtended Reality, Artificial Intelligence and Neural Engineering (MetroXRaine) tenutosi a St Albans (UK) nel 21-23 October 2024) [10.1109/metroxraine62247.2024.10796786].

Availability:

This version is available at: 11583/2996958 since: 2025-02-04T07:08:07Z

Publisher:

IEEE

Published

DOI:10.1109/metroxraine62247.2024.10796786

Terms of use:

This article is made available under terms and conditions as specified in the corresponding bibliographic description in the repository

Publisher copyright

(Article begins on next page)

Next Generation Memristor Reservoir Computing

K.Nikiruy, T.Ivanov, M. Ziegler
Department of Electrical Engineering
and Information Technology
Micro- and Nanoelectronic Systems TU
Ilmenau
Ilmenau, Germany
Kristina.Nikiruy@tu-ilmenau.de

D. Rossetti, F. Corinto, A. Ascoli
Department of Electronics and
Telecommunications (DET)
Politecnico di Torino
Turin, Italy
davide.rossetti@polito.it

R. Tetzlaff, A.S. Demirkol, N. Schmitt
Faculty of Electrical and Computer
Engineering Institute of Circuits and
Systems TU Dresden
Dresden, Germany

Abstract—The nonlinear transformation used in reservoir computing can be effectively replaced by nonlinear vector autoregression (NVAR) for data prediction. In such a method, also known as next generation reservoir computing (NGRC), the input signal consists of a linear part, including several previous data points, and their nonlinear combinations. Here we show that the application of this method to a network with memristive weights (memristors) can be used to predict signals, depending on the nature of the nonlinear functions and the number of memristors. The network allows an accurate prediction of chaotic time series of Mackey-Glass and Duffing oscillators.

Keywords—Memristor, Reservoir Computing, Nonlinear Vector Autoregression, Machine Learning

I. INTRODUCTION

In the field of unconventional computing, a wide variety of methods are used to process unknown and complex data, which can be roughly divided into statistical methods and machine learning methods [1,2]. While the use of statistical methods already has a long tradition, machine learning (ML) has gained more and more importance in recent years as it has been able to demonstrate its potential impressively [3]. There are many different methods in this area, with Reservoir Computing (RC) attracting a lot of attention in recent years due to its simple structure and feasibility in hardware [4].

Recently, the possibility of a synergetic connection between RC and the field of statistical methods was investigated by Gauthier et al. [5], which introduced a new paradigm named Next Generation Reservoir Computing (NGRC). These methods, however, do not use a reservoir for implementing the nonlinear transformation of the inputs. They directly operate on the input data, particularly on what is referred to as the feature vector. NGRC uses correlations, involving the feature vector, together with the Tikhonov regularization method to generate a suitable nonlinear transformation of the input data similar to a standard reservoir [5].

However, the NGRC method requires the optimization of the type and number of nonlinearities in the feature vector, which can be a more difficult task than the process of fine tuning the reservoir parameters, especially for the case where little is known about the input data set [6]. In this context, the use of nonlinear circuit elements, and memristors in particular, can address this issue [7,8], since on the one hand they can produce an appropriate nonlinear and tunable representation of the input data, when integrated in a suitable circuit topology [9], and on the other hand they allow for an efficient and

compact realization of the signal processing concept in hardware [10].

In this article, we look at the prerequisites for realizing the NGRC within hardware based on memristors. For this purpose, relevant properties of our non-volatile memristors, to be leveraged for this application, are identified through a theoretico-experimental investigation based on physically-realized memristors. For this purpose, Mackey–Glass and Duffing equations have been used as a benchmark to explore the beneficial effect of the memristors' nonlinearities on the prediction of chaotic time series. Furthermore, the advantages and disadvantages of the NGRC are discussed and an outlook on possible research developments is given.

II. NEXT GENERATION MEMRISTIVE RESERVOIR COMPUTING

The concept of proposed next generation memristor reservoir computing (NGMemRC) scheme is schematically shown in Fig. 1. This network uses the ideas of Gauthier et al [5] to use autoregression for computing and also leverages special properties of memristors, specifically the non-volatile data storage capability and the state-dependent nonlinearity in the current voltage relationship. In the sections to follow, we will present the computational framework, which inspires our research approach, and the promising results of the first scientific investigations. To this end, we will first describe the properties of our memristors and explain how technological developments in material science may allow to tune the nonlinearity in their state-dependent current-voltage relationship. The nonlinearity in the state-dependent input-output behaviour of the memristors, currently available in our labs, was exploited for the development of the NGMemRC concept. The potential of the concept is demonstrated in section III through numerical simulations of two benchmark problems for the prediction of chaotic time series, related, particularly, to the solutions of the time-delayed Mackey–Glass equation and of the Duffing oscillator equation.

A. Transition Metal-oxide Memristor Devices

The adjustment of nonlinearities in the current-voltage behavior of memristors is a key task in tailoring the devices for use in neuromorphic systems. In that respect, multilayer transition metal oxides are an interesting material class, since they allow precise adjustment of resistance switching characteristics and current-voltage nonlinearity [11,12].

Fig. 2a shows a memristor device stack that features the layer sequence TiN/TiO₂/Al₂O₃/HfO_x/Au. Within the functional film, the HfO_x top layer is endows the device with a memristive character, the Al₂O₃ modifies the interfacial properties, while the TiO₂ bottom layer forms well-defined

* Funded by the Deutsche Forschungsgemeinschaft (DFG, German Research Foundation) – Project RECOMMEND Project number 536063366 as part of the DFG priority program SPP 2262 MemrisTec – Project number 422738993 and the Carl-Zeiss Foundation – Project MemWerk.

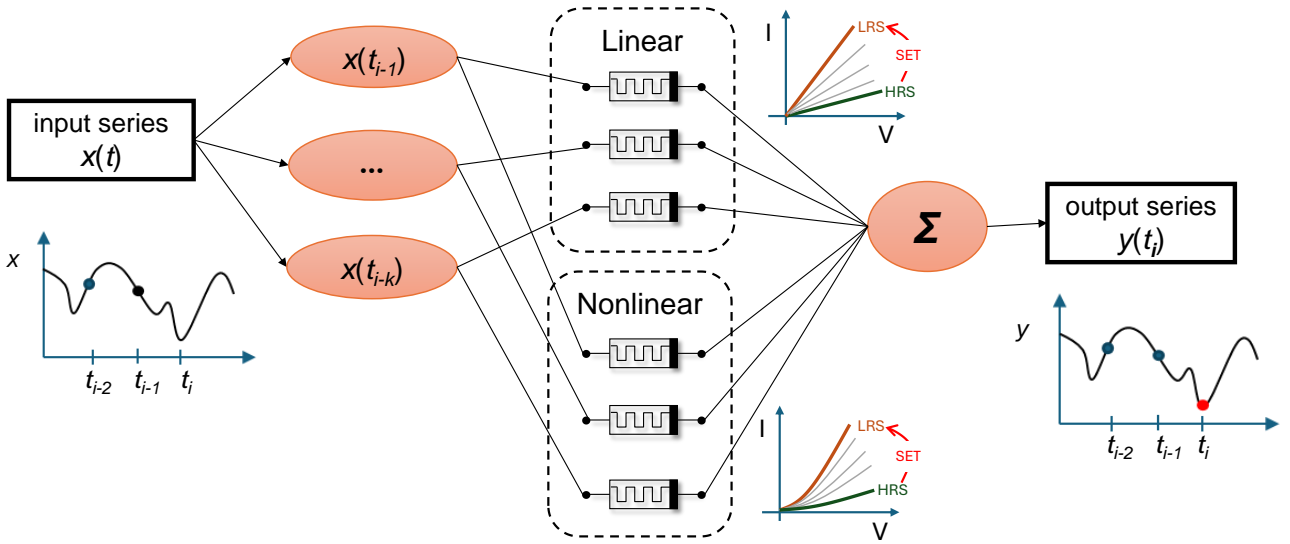


Fig. 1: Next Generation Memristor Reservoir Computing (NGMemRC): illustrative sketch of the proposed computational framework, envisaging the use of a memristive network to perform a nonlinear autoregression on the feature vector to predict chaotic time series. Following the NGRC model [5] the network uses an input vector of time-delay states, whose components are k past samples of the input time series $x(t)$, namely samples $x(t_{i-1}), \dots, x(t_{i-k})$. The linear and nonlinear transformation of adaptive weights in the output layer are provided by the (non-)linear current-voltage (I-V) characteristics of memristive devices.

interfaces with the TiN electrode and the AlO_3 layer. The resistive switching behavior was tailored through the stoichiometry of HfO_x ($x = 1.8, 2$) and through its operating conditions. We have recently shown that the resistive switching mechanism can be tuned from area-type to filament-type, which triggers different nonlinearities in the I-V characteristics [11]. In particular, for sub-stoichiometric $\text{HfO}_{1.8}$, a transition from area to filament type switching is possible, while for stoichiometric HfO_2 , area type switching is found to feature a robust character even at higher electrical voltages [12]. Fundamental here is the role of the Al_2O_3 layer, which stabilizes the area-type switching by controlling the formation of oxygen vacancies at the $\text{Al}_2\text{O}_3/\text{HfO}_x$ interface [12]. As we have shown in reference [12], such devices combine multi-level analogue switching, linear resistance change and long retention times without external current compliance and initial electroforming cycles.

Having preliminarily acquired a deep knowledge of the properties of our memristors, we have later on integrated them into passive crossbar structures. In particular, memristors were fabricated in a 4-inch wafer thin-film technology. The memristors were arranged on the wafer in crossbar arrays with different dimensions. An array with 25×25 cells is shown in Fig. 2(b). The crossbar structure dimensions and the switching mechanism of the memristive devices were adapted in such a way that each device does not influence any other for the realization of matrix-vector multiplications. The individual cells were separated by a sufficiently wide SiO_2 insulation layer (see Fig. 2(a)).

To demonstrate the functionality of the memristive crossbar structures, a 25×25 crossbar array was measured. Fig. 2c shows the results obtained for two resistance states at 1.5 V, labelled HRS (high resistance state) and LRS (low resistance state). A representative I-V curve of a single memristor cell within the crossbar is shown in Fig. 2(d). Furthermore, as shown in the inset of Fig. 2(d) the experimentally-acquired

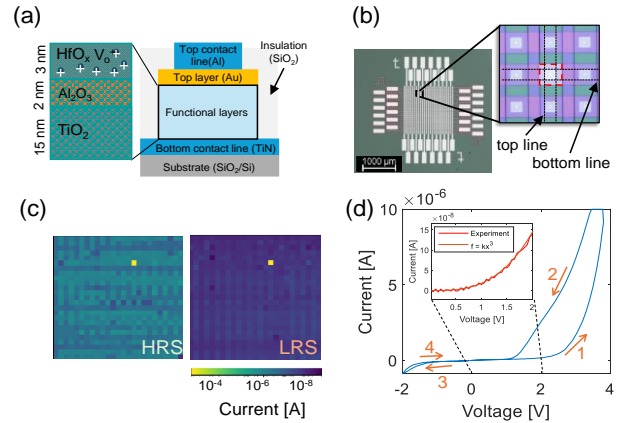


Fig. 2: Fabricated memristors: (a) Cross sectional sketch of a single memristor cell with functional layers arranged in the stack $\text{HfO}_x/\text{Al}_2\text{O}_3/\text{TiO}_2$. (b) Optical microscope image displaying a fabricated crossbar array with 25×25 memristors. (c) Heatmaps showing the distributions of the HRS and of the LRS across a 25×25 crossbar array. (d) Representative I-V curve of a single memristor cell within the crossbar. Inset: Nonlinear current-voltage relation of the memristors to realize the nonlinear transformation of the feature vector in the computing scheme illustrated in Fig. 1.

current data, associated to the HRS, yet covering only the voltage range [0V, 2V], were fitted through a cubic polynomial in order to exploit the memristor nonlinearity in the output layer of the proposed system in the investigations to be discussed next.

B. NGMemRC - Paradigm

The proposed memristor-based computing scheme is based on the NGRC concept discussed in reference [5]. In contrast to classical reservoir computing, the inputs of the NGRC are fed as in an autoregressive network. Particularly, in order to predict the sample $x(t_i)$ an input vector \mathbf{X} of size k is first constructed using the previous k samples $x(t_{i-1}), \dots, x(t_{i-k})$ of the time series $x(t)$ itself. Multiplying this vector simultaneously with a vector \mathbf{W}_L of linear memristive weights

and with a vector \mathbf{W}_{NL} of nonlinear memristive weights, and then summing up the respective scalar results, the output y of the system at time t_i may be cast as:

$$y(t_i) = \mathbf{W}_L \cdot \mathbf{X} + \mathbf{W}_{NL}(\mathbf{X}) \cdot \mathbf{X}. \quad (1)$$

The j^{th} components of the vectors \mathbf{W}_L and \mathbf{W}_{NL} is equal to the normalized $G_L(m_j^L)$ and $G_{NL}(m_j^{NL}, V)$, that denotes the memductance of the memristor M_j^L , sitting in the j^{th} position across the linear device column, and the memductance of the memristor M_j^{NL} , sitting in the j^{th} position across the nonlinear device column from Fig.1, where V denotes applied voltage. The scalar memory states m_j^L, m_j^{NL} are assumed to be fixed at all times during operation. Essentially, for each $j \in \{0, 1, \dots, k\}$, the memristor M_j^L , (M_j^{NL}) acts as a linear resistor (as a nonlinear voltage-controlled resistor) during operation, as the voltage $V \sim x(t_{i-j})$, falling across it, is rigorously kept below its maximum read voltage to avoid the corruption of its memory state over time. The memristors M_j^L, M_j^{NL} are assumed to admit memductance functions of the form:

$$G_L(m_j^L) = m_j^L \text{ and } G_{NL}(m_j^{NL}, V) = m_j^{NL} f(V). \quad (2)$$

Since V in the here considered model can be directly identified with the time delayed input signals $x(t_{i-j})$, we obtain the following relationship:

$$\mathbf{W}_L = [w_1^L \dots w_k^L] \quad (3)$$

and

$$\mathbf{W}_{NL} = [w_1^{NL} f(x(t_{i-1})) \dots w_k^{NL} f(x(t_{i-k}))] \quad (4)$$

This allows us to write the prediction of the NGMemRC system as an autoregression with optimized weighting coefficients w_j^L (linear part) and w_j^{NL} (nonlinear part):

$$y(t_i) = \sum_{j=1}^k w_j^L x(t_{i-j}) + \sum_{j=1}^k w_j^{NL} f(x(t_{i-j})) x(t_{i-j}), \quad (5)$$

In the latter equation $f(x(t_{i-k})) = x(t_{i-k})^2$ is a quadratic nonlinearity, extracted from the current versus voltage locus of the memristor, similarly as shown in Fig. 2(d).

The memristive weights are optimized through a suitable learning procedure. In particular, using training part of the time series $x(t)$, specifically the first i samples, two voltage-dependent matrices of dimension $(i-k) \times k$, named \mathbf{S}_L and \mathbf{S}_{NL} , are constructed from samples of the data portion under consideration as:

$$\mathbf{S}_L = \begin{pmatrix} x(t_k) & \dots & x(t_1) \\ \vdots & \ddots & \vdots \\ x(t_{i-1}) & \dots & x(t_{i-k}) \end{pmatrix} \quad (6)$$

and

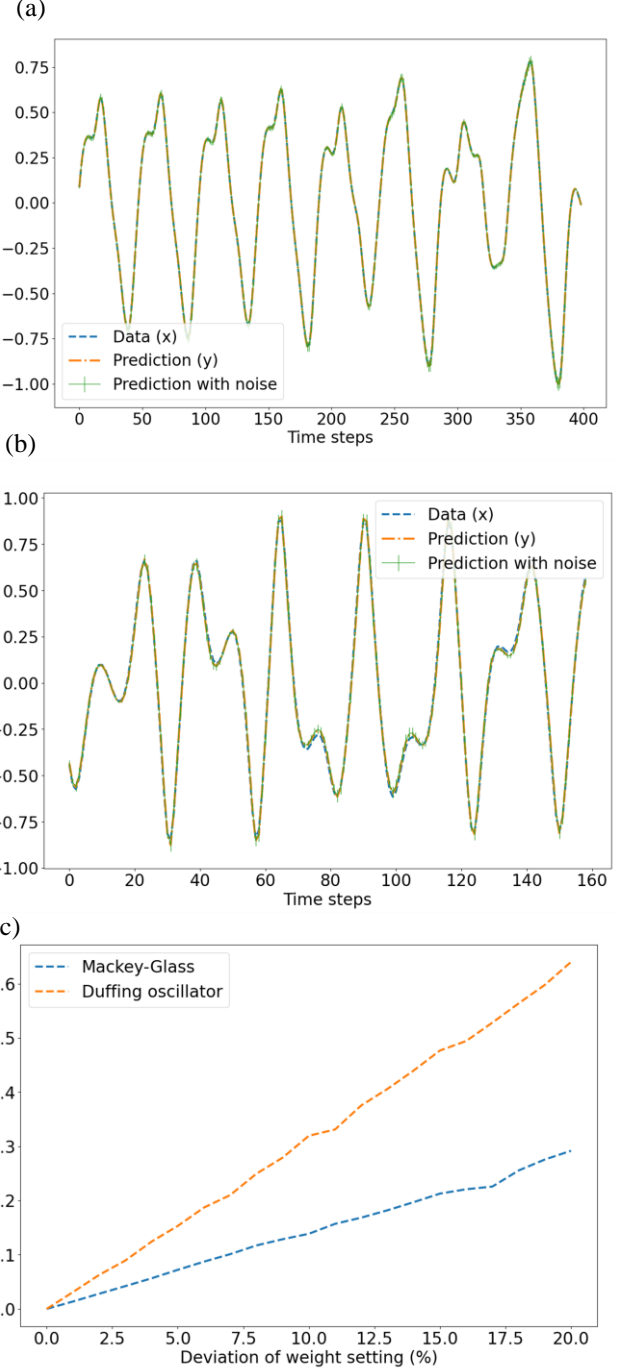


Fig. 3. One-step-ahead prediction of chaotic time series, extracted from numerical simulations of the time-delayed Mackey-Glass equation (a) and of the Duffing oscillator equation (b), as resulting from the network of Fig. 1 employing only the linear memristors. In case noise displaces the memristors' conductances away from the nominal values, set optimally through the training process, as explained in the text, some degradation in the prediction accuracy is observed, when assuming a variation in the synaptic weights according to a normal distribution with a variance σ versus average μ ratio of 0.01. This may be better inferred from plot (c), which shows the average deviation of the predicted data from the target time series as a function of the maximum displacement of the synaptic weights from the nominal values.

$$\mathbf{S}_{NL} = \begin{pmatrix} f(x(t_k))x(t_k) & \dots & f(x(t_1))x(t_1) \\ \vdots & \ddots & \vdots \\ f(x(t_{i-1}))x(t_{i-1}) & \dots & f(x(t_{i-k}))x(t_{i-k}) \end{pmatrix} \quad (7)$$

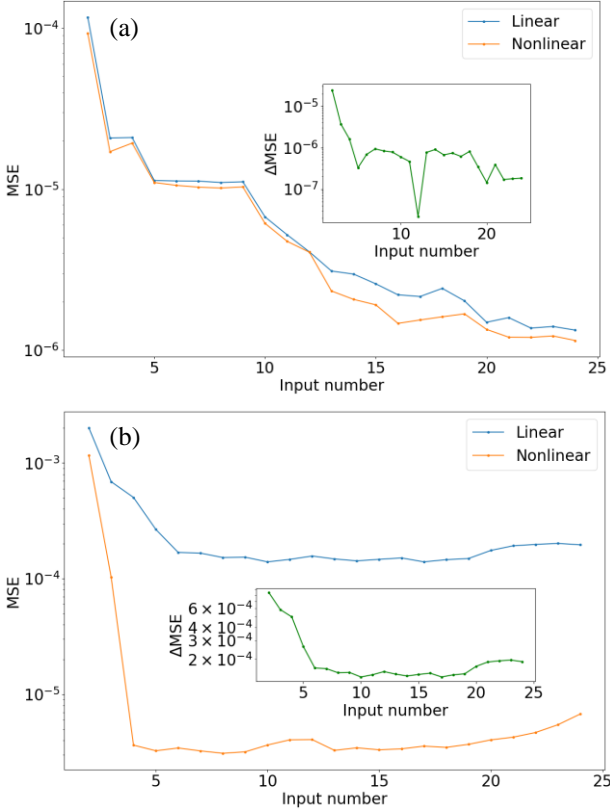


Fig. 4. Mean Squared Error (MSE) in the prediction of the chaotic time series extracted from numerical simulations of the time-delayed Mackey-Glass equation (a) and of the Duffing oscillator equation (b) as a function of the number k of past samples of the input signal $x(t)$ embedded in the feature vector for forecasting its next datapoint. As shown through the orange trace, employing a column of k nonlinear memristors, besides the column of k linear memristors, within the proposed NGMemRC network of Fig. 1 allows to improve the data series prediction accuracy over the case where k linear memristive synapses are employed (refer to the blue trace), especially in the Duffing oscillator problem. The insets in the two plots illustrate the reduction ΔMSE in the MSE, enabled by the exploitation of the nonlinearity of the memristors, as a function of the length of the input vector.

respectively. Defining a composite matrix \mathbf{S} of dimension $(i-k) \times 2 \cdot k$ as $\mathbf{S} = [\mathbf{S}_L \mathbf{S}_{NL}]$, the weights of the $2 \cdot k$ linear and nonlinear memristors are trained via ridge regression according to the formula:

$$\mathbf{W} = (\mathbf{S}^T \mathbf{S} + \gamma \mathbf{I})^{-1} \mathbf{S}^T \mathbf{y}_T \quad (8)$$

where the vector \mathbf{W} combines \mathbf{W}_L and \mathbf{W}_{NL} , while \mathbf{y}_T denotes a $(i-k)$ target output vector, \mathbf{I} is identity matrix, γ denotes regularization parameter.

In case only the column of k linear memristors were used in the network of Fig. 1 (see section III), the training of their synaptic weights would be based on the very same samples of $x(t)$, aiming at the prediction of the very same target vector \mathbf{y}_T , but the ridge regression formula would reduce to:

$$\mathbf{W}_L = (\mathbf{S}_L^T \mathbf{S}_L + \gamma \mathbf{I})^{-1} \mathbf{S}_L^T \mathbf{y}_T \quad (9)$$

C. Learning tasks: chaotic time series

The proposed next generation memristor reservoir computing scheme has been applied for time series prediction. In particular, we tested it on two benchmark problems, requiring to forecast the chaotic solutions of the Mackey-Glass equation and of the Duffing oscillator equation, respectively. The Mackey-Glass equation is given by:

$$\frac{dx(t)}{dt} = \beta \frac{x(t-\tau)}{1+x(t-\tau)^n} - \gamma x(t) \quad (10)$$

with the positive constants β , γ and n and the time delay τ defining the chaotic time evolution of variable $x(t)$. In the following investigation the parameters have been chosen as $\beta=2$, $\gamma=1$, $n=10$, and $\tau=17$.

As a second application test, we used the Duffing oscillator equation. Solving the second-order ordinary differential equation:

$$\ddot{x} + \delta \dot{x} + \alpha x + \beta x^3 = \gamma (\cos \omega_1 t + \cos \omega_2 t) \quad (11)$$

a chaotic time series for the state variable x was generated when the parameters were taken as $\alpha=1$, $\beta=0.1$, $\gamma=4$, $\delta=0.02$, $\omega_1=1.0$, $\omega_2=1.1$. Both datasets were normalized to the range $[-1;1]$.

III. RESULTS AND DISCUSSION

In a first set of simulations, we used two k -long vector of linear weights. Under this assumption, plots (a) and (b) in Fig. 3 show the chaotic time series prediction of the NGMemRC network from Fig. 1 for the Mackey-Glass and Duffing oscillator equations, respectively. The prediction of the data point $x(t_i)$, of the time series is based upon the previous 5 samples $x(t_{i-1})$, $x(t_{i-2})$, $x(t_{i-3})$, $x(t_{i-4})$, $x(t_{i-5})$ of the time series of $x(t)$ itself. Interestingly, the use of just 5 past samples besides the current sample is sufficient to predict rather accurately the next data point in both the benchmark problems under focus. Clearly, the hardware realization of a simple open-loop memristive network of this kind requires little effort from the circuit designer, revealing the potential of the proposed data processing paradigm in artificial intelligence applications. Solving the same data prediction task employing the classical reservoir computing approach would require the use of a significantly larger number of components in the hardware realization. Including the intrinsic variability sources, affecting the electrical behavior of a memristive device at any point in time, in the numerical investigations, by allowing a variation in the memristive synaptic weights according to a normal distribution with a variance σ versus mean value μ ratio of 0.01, the data prediction capability of the proposed NGMemRC

network deteriorated somehow. This deterioration is reflected in the green traces, illustrating noise-corrupted prediction data averaged over 1000 simulation runs, and to the error bars, crossing the traces vertically at regular time intervals, and showing the range of values among the set of 1000 predictions at the respective time steps, in Figs. 3(a)-(b). Assuming a 1% deviation in the synaptic weight setting resulted in a reduction of less than 5% in the accuracy of the

data series prediction, which sheds light into the potential robustness of the proposed computational paradigm. However, despite recent experimental findings on how to drastically reduce variability in certain memristors integrated on CMOS [13], attaining precise control on the conductance of a resistance switching device is in general still an open problem in nanotechnology, and thus exploring the effect of synaptic weight inaccuracy on the performance of the proposed computing system is of utmost importance. As shown in Fig. 3(c), the average deviation of the predicted time series from the target data increases linearly with the maximum displacement of the memristor conductance from the nominal value in both benchmark problems. However, the sensitivity of the NGMemRC network to noise is higher in the Duffing oscillator problem.

In order to assess the beneficial effect of the memristor nonlinearity (refer to section II.A) on the proposed computational framework, for each of the two benchmark problems under focus, the chaotic time series prediction capability of the network of Fig. 1 was tested in two different scenarios, specifically once in case the network employs only k memristors, assumed to act as linear resistors, and once in case the network employs a first column of k memristors, assumed to act as linear resistors, as well as a second column of k memristors, assumed to act as nonlinear voltage-controlled resistors. Let us define the mean square error (MSE) in the time series prediction as:

$$\text{MSE} = \frac{1}{N} \sum_{i=1}^N (x_i - y_i)^2 \quad (12)$$

where x_i and y_i are the data points of the actual and predicted time series at time t_i , respectively, and N is the total number of time steps. In the following, by input number we refer to the number k of past samples of the time series of $x(t)$ included in the feature vector together with the current sample for forecasting its next data point. On the basis of the discussions in section II.B, the predictions of the chaotic time series at time t_i in the first and second scenario are respectively computed via:

$$y(t_i) = \sum_{j=1}^k w_j^L x(t_{i-j}) \quad (13)$$

and

$$y(t_i) = \sum_{j=1}^k w_j^L x(t_{i-j}) + \sum_{j=1}^k w_j^{NL} x(t_{i-j})^3. \quad (14)$$

Plots (a) and (b) in Fig. 4 depict the MSE in the prediction of the chaotic time series of the time-delayed Mackey-Glass and Duffing oscillator equations, respectively, as a function of the number k of past samples of the state variable itself embedded into the feature vector together with its current sample for forecasting its next data point, according to the realization based upon the proposed NGMemRC network. The blue trace refers to the scenario, where the network employs k linear memristors. The orange trace refers to the scenario, where the network employs k linear memristors and k nonlinear memristors. Clearly, exploiting the cubic current versus voltage relationship of the nonlinear memristors allows to improve the accuracy of the chaotic time series prediction, for a given value assigned to k , relative to the case where the network employs k linear memristors, only. Of course, the

larger is the input number and the better is the performance of the network. In the time series prediction of the time-delayed Mackey-Glass equation, the MSE keeps decreasing with the input number, and at least 15 past samples of $x(t)$ need to be included in the feature vector together with its current sample for an accurate forecast of its next data point (refer to plot (a)). On the other hand, setting k to 5 is sufficient in the Duffing oscillator problem to observe the descent of the MSE to a saturation plateau (see plot (b)). To better appreciate the advantages, which the nonlinearity of the memristors provides to the computational paradigm, the insets in Fig. 4 show the reduction ΔMSE (the difference of MSE in the linear and nonlinear case) in the chaotic time series prediction. The reduction originates from the use of $2k$ memristors, of which half are nonlinear, in place for the adoption of k linear memristors only, for both the benchmark problems under the zooming lens in this manuscript. Future research investigations shall be aimed at exploring the potential of leveraging higher-order memristor nonlinearities for improving the accuracy of the NGMemRC network in solving time series prediction problems under a variety of learning methods, including the gradient descent technique. These preliminary studies shall pave the way to a conscious and systematic design of a robust, area- and energy-efficient hardware realization of the proposed computational paradigm.

IV. CONCLUSION

In this paper, we describe a methodology for developing new systems that combine the energy efficiency of vector-matrix multiplications, computed across memristive crossbars, with the tunability of autoregressive methods for improving the accuracy and reducing the computational efforts in time series predictions. Employing as exemplary case studies the Mackey-Glass and Duffing ordinary differential equation systems, we show that a network, performing a linear vector autoregression, is able to predict chaotic time series even when the potentially-detrimental effect of the variability in the electrical behaviours of different memristor samples, expected to be matched one to the other, as well as the variability in the electrical behaviour of a single device sample from cycle to cycle are taken into account. On the other hand, it is possible to utilize the inherent nonlinearities in the input-output behaviours of memristive devices to improve the accuracy of time series predictions. The simulations show the promising potential of the implementation of autoregressive methods in memristive hardware.

REFERENCES

- [1] Jaurigue, L., & Lüdge, K. (2022). Connecting reservoir computing with statistical forecasting and deep neural networks. *Nature Communications*, 13(1), 227.
- [2] Ij, H. (2018). Statistics versus machine learning. *Nat Methods*, 15(4), 233.
- [3] Silver, D. et al. (2016). Mastering the game of Go with deep neural networks and tree search. *Nature*, 529(7587), 484-489.
- [4] Jaeger, H. (2001). The ‘‘echo state’’ approach to analysing and training recurrent neural networks-with an erratum note. Bonn, Germany: German National Research Center for Information Technology GMD Technical Report, 148(34), 13.
- [5] Gauthier, D. J., Bollt, E., Griffith, A., & Barbosa, W. A. (2021). Next generation reservoir computing. *Nature communications*, 12(1), 5564.

- [6] Jaurigue, L., Robertson, E., Wolters, J., & Lüdge, K. (2021). Reservoir computing with delayed input for fast and easy optimisation. *Entropy*, 23(12), 1560.
- [7] Du, C., Cai, F., Zidan, M. A., Ma, W., Lee, S. H., & Lu, W. D. (2017). Reservoir computing using dynamic memristors for temporal information processing. *Nature communications*, 8(1), 2204.
- [8] Moon, J., Ma, W., Shin, J. H., Cai, F., Du, C., Lee, S. H., & Lu, W. D. (2019). Temporal data classification and forecasting using a memristor-based reservoir computing system. *Nature Electronics*, 2(10), 480-487.
- [9] F. Corinto, M. Forti, and L.O. Chua, "Nonlinear Circuits and Systems with Memristors - Analogue Computing via the Flux-Charge Analysis Method," Springer, 2020, ISBN-13: 978-3-030-55650-1.
- [10] Escudero, M., Spiga, S., Di Marco, M., Forti, M., Innocenti, G., Tesi, A., Corinto, F., and Brivio, S. (2022, September). Physical Implementation of a Tunable Memristor-based Chua's Circuit. In *ESSCIRC 2022-IEEE 48th European Solid State Circuits Conference (ESSCIRC)* (pp. 117-120). IEEE.
- [11] S. Park, S. Klett, T. Ivanov, A. Knauer, J. Doell, and M. Ziegler, "Engineering Method for Tailoring Electrical Characteristics in TiN/TiO_x/HfO_x/Au Bi-Layer Oxide Memristive Devices," *Frontiers in Nanotechnology*, vol. 3, no. 670762, 16pp., 2021.
- [12] S. Park, B. Spetzler, T. Ivanov, and M. Ziegler, "Multilayer redox-based HfO_x/Al₂O₃/TiO₂ memristive structures for neuromorphic computing," *Scientific Reports*, vol. 12, no. 18266, 15pp., 2022.
- [13] Rao, M., Tang, H., Wu, J. et al. "Thousands of conductance levels in memristors integrated on CMOS." *Nature*, vol. 615, 823-829, 2023. <https://doi.org/10.1038/s41586-023-05759-5>